HIPPOCAMPUS 16:1026–1031 (2006)

RAPID COMMUNICATION

From Grid Cells to Place Cells: A Mathematical Model

Trygve Solstad,[1] Edvard I. Moser,[1] and Gaute T. Einevoll[2]

ABSTRACT: Anatomical connectivity and recent neurophysiological results imply that grid cells in the medial entorhinal cortex are the principal cortical inputs to place cells in the hippocampus. The authors propose a model in which place fields of hippocampal pyramidal cells are formed by linear summation of appropriately weighted inputs from entorhinal grid cells. Single confined place fields could be formed by summing input from a modest number (10–50) of grid cells with relatively similar grid phases, diverse grid orientations, and a biologically plausible range of grid spacings. When the spatial phase variation in the grid-cell input was higher, multiple, and irregularly spaced firing fields were formed. These observations point to a number of possible constraints in the organization of functional connections between grid cells and place cells. © 2006 Wiley-Liss, Inc.

KEY WORDS: hippocampus; place cells; entorhinal cortex; grid cells; spatial representation; memory

The hippocampus is thought to be part of a widespread brain network for spatial representation and navigation (O'Keefe and Nadel, 1978). A principal cell type of this network is the hippocampal "place cell," which, when the animal is awake, discharges if and only if the animal is within a confined region of the environment, the "place field" of the neuron (O'Keefe and Dostrovsky, 1971). In open environments place fields can be approximated by a Gaussian function (Muller et al., 1987; O'Keefe and Burgess, 1996) with a diameter increasing from less than 20 cm in some cells in the dorsal hippocampus (Muller et al., 1987; Kjelstrup et al., 2006) to more than 50 cm in the intermediate region of the hippocampus (Jung et al., 1994; Maurer et al., 2005) and several meters in the most ventral region (Kjelstrup et al., 2006). Most, but not all, place cells have a single firing field in a standard-sized experimental environment. The spatial representation of hippocampal place cells is nontopographical, i.e., neighboring cells fire in different regions of the environment and the location of the animal can thus be represented accurately by the collective activity of any local ensemble of place cells (Wilson and McNaughton, 1993).

Principal cells in the medial entorhinal cortex (MEC) also signal an animal's location in that each cell is characterized by multiple firing fields arranged in a strikingly regular, triangular, grid-like pattern that tessellates any two-dimensional environment explored by the animal (Hafting et al., 2005). The firing pattern of each "grid cell" can be characterized by its spacing (the distance between neighboring vertices of the grid), orientation relative to the environment, and spatial phase (the offset relative to a fixed position in the environment). The spacing of the grid increases from the dorsal to the ventral end of MEC (Fyhn et al., 2004; Hafting et al., 2005; Sargolini et al., 2006). Grid cells recorded at the same dorsoventral level have similar spacings and orientations but, as for place cells in the hippocampus, the actual firing locations (spatial phase) of neighboring neurons are distributed, i.e., all locations in the environment are represented within a local ensemble of grid cells. Unlike place cells in the hippocampus, grid cells are active in all environments, regardless of external cues, suggesting that these cells are part of a universally applicable, internally generated map of the spatial environment (Hafting et al., 2005; McNaughton et al., 2006).

Any localized function, like a place field, can be constructed from a linear sum of oscillatory patterns of multiple scales (Riley et al., 2006). Several studies show that hippocampal pyramidal neurons perform linear summation of synaptic inputs (Cash and Yuste, 1998, 1999; Gasparini and Magee, 2006). Because grid cells are only one synapse upstream of the hippocampus, direct dendritic summation of grid-cell input appears as an attractive model for the emergence of hippocampal place fields. The aim of the present study was to investigate how grid-cell inputs must be arranged in terms of number of afferent inputs, grid spacings, grid orientations, and grid phases, to produce realistic place fields in the CA3 and CA1 subfields of the hippocampus.

In our model the net somatic activity level (e.g., somatic potential) in a hippocampal place cell is expressed as a weighted sum of excitatory inputs from a set of N grid cells with some additional spatially unspecific inhibition C_{inh} to balance the excitation. A simple model for place-field generation is thus (Fig. 1A):

$$f(x,y) = \left[\sum_{n=1}^{N} A_{\mathbf{w}}^{n} g_{\mathbf{w}}^{n}(x,y) - C_{\text{inh}}\right]_{+} \qquad (1)$$

The subscript $\mathbf{w} = (\lambda, \Theta, \boldsymbol{r}_0)$ specifies the spacing λ, orientation Θ, and spatial phase $\boldsymbol{r}_0 = [x_0, y_0]$ of the

[1] **Center for the Biology of Memory, Norwegian University of Science and Technology, Trondheim, Norway;** [2] **Department of Mathematical Sciences and Technology and CIGENE, Norwegian University of Life Sciences, Ås, Norway**
This article contains Supplementary material available at http://www.interscience.wiley.com/jpages/1050-9631/suppmat.
*Correspondence to: Edvard Moser, Centre for the Biology of Memory, Olav Kyrres gt 9, 7489, Trondheim, Norway. E-mail: edvard.moser@cbm.ntnu.no
Accepted for publication 28 September 2006
DOI 10.1002/hipo.20244
Published online 8 November 2006 in Wiley InterScience (www.interscience.wiley.com).

contributing grid cells, $g^n_{\mathbf{w}}(x,y)$ is the grid-cell function for the n'th grid cell, and $A^n_{\mathbf{w}}$ is the corresponding weight coefficient (mainly determined by the synaptic weight and projection density of each grid cell). To avoid negative firing rates we use the half-wave rectification operation in the conversion from somatic activity to firing rate, i.e., $[z]_+ = z$ for $z \geq 0$ and 0 otherwise.

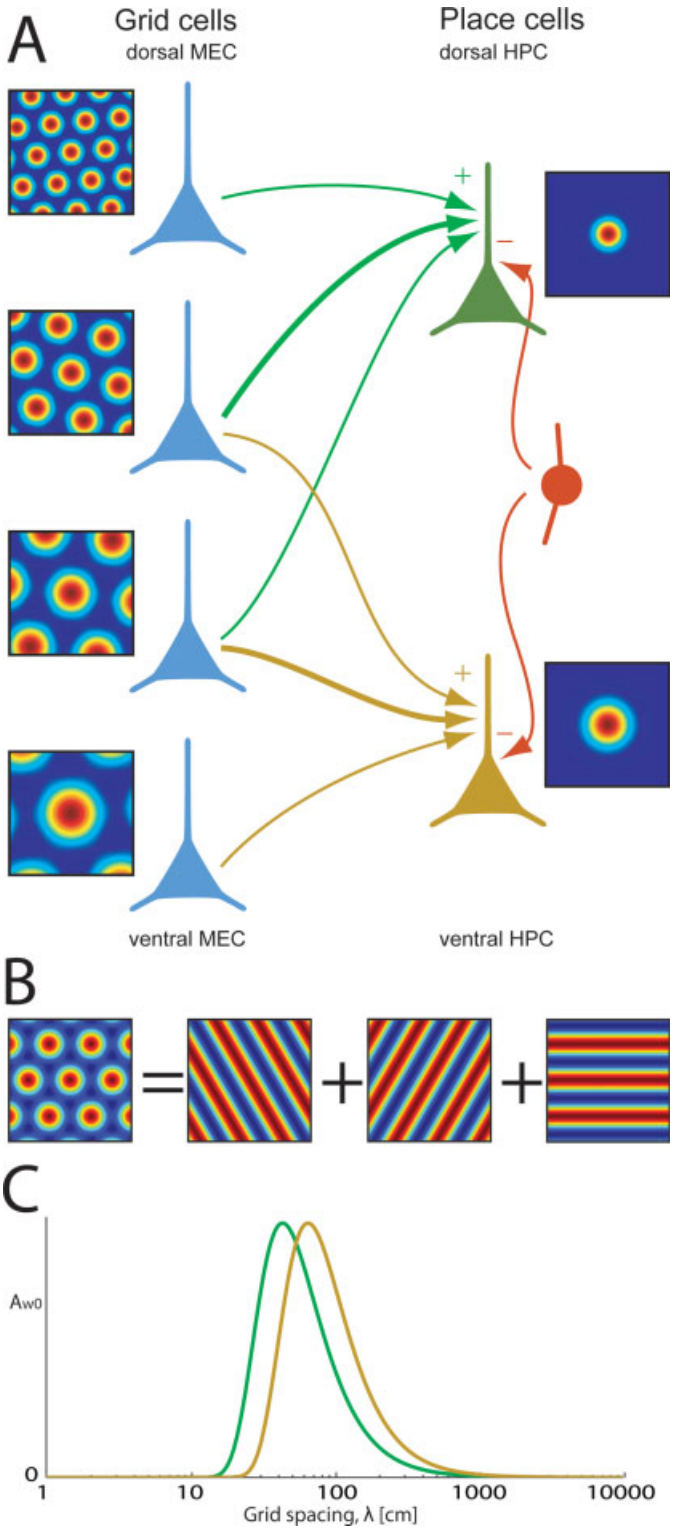

The grid-cell functions $g_{\mathbf{w}}(x,y)$ are constructed from a sum of three two-dimensional sinusoidal gratings, specified by their wave vectors $\boldsymbol{k}$, with 60 and 120 degree angular differences as shown in Figure 1B, and adjusted to take firing-rate values between 0 and $g^{\max}_{\mathbf{w}}$ (Supplementary material, Section 1):

$$g_{\mathbf{w}}(x,y) = g^{\max}_{\mathbf{w}} \frac{2}{3}\left(\frac{1}{3}\sum_{i=1}^{3}\cos(\boldsymbol{k}_i(\mathbf{r}-\mathbf{r}_0)) + \frac{1}{2}\right) \qquad (2)$$

Because the grid-cell functions are formulated in terms of harmonic functions, Fourier theory suggests an analytical expression for how much each grid cell should contribute to a specific place field. For a Gaussian place field, $f(x,y) = f^{\max}\, e^{-(x^2+y^2)/\sigma^2}$, it is sufficient to include grid cells with identical spatial phase (Riley et al., 2006). If grid spacings are sampled logarithmically, the weight function

$$A_{\mathbf{w0}} = \frac{f^{\max}}{g^{\max}_{\mathbf{w0}}} 2\pi\sigma^2 \frac{e^{-\frac{4}{3}\pi^2\sigma^2/\lambda^2}}{\lambda^2} \frac{2\pi}{N}\ln(\lambda_{\text{upper}}/\lambda_{\text{lower}}) \qquad (3)$$

is derived for Eq. (1) (Fig. 1C; Supplementary material, Section 2). The altered subscript "**w0**" signals that only grid cells with a single spatial phase (i.e., $\boldsymbol{r}_0 = [0,0]$) are considered. λ_{lower} and λ_{upper} denote the lower and upper spacing allowed in the sum. In the ideal case with an infinite number of contributing grid cells covering all orientations and all spacings ($\lambda_{\text{lower}} = 0$, $\lambda_{\text{upper}} \to \infty$), this choice of weights for Eq. (1) gives rise to the perfectly Gaussian place fields with maximum firing rate $f^{\max}$ depicted in Figure 1A (see also Supplementary material, Section 2). The parameter σ with dimension length characterizes the size of

FIGURE 1. Model for place-field formation. (A) Assumed anatomical connectivity between grid cells in the medial EC (MEC) and place cells in the hippocampus. Grid cells (blue) are illustrated with small grid spacings in the dorsal pole of MEC and with larger grid spacings at more ventral levels. All place cells with a place field receive input from grid cells of similar spatial phase (a common central peak) but a diversity of spacings and orientations. Hippocampal place cells with a small firing field (green) are innervated by grid cells from more dorsal parts of the EC than place cells with a larger field (yellow). Connection weights are indicated by the thickness of the arrows. Interneurons (red) provide nonspecific inhibition to keep overall firing rates at physiological levels. The color code for the rate maps ranges from blue (0 Hz) to red (peak rate). (B) Grid functions are constructed from a sum of three sinusoidal grating functions with 60 and 120 degrees angular difference, and can take any specified spatial phase, orientation, and spacing, see Eq. (2). (C) Distribution of input weight from grid cells projecting to a place cell with a Gaussian place field as a function of the logarithm of the spacing, i.e., A_{w0} in Eq. (3) (weight is independent of grid orientation). Green curve: σ = 12 cm. Yellow curve: σ = 18 cm. Note that the weight distributions for the two place fields have identical shapes, but the distribution for the large place field is shifted towards larger grid spacings. For the small field, the maximum contribution comes from a grid input with a spacing of $\lambda_{\max}$ = 43.5 cm; for the large field the corresponding grid spacing is $\lambda_{\max}$ = 65.3 cm. Also note that to form significantly larger place fields (as recorded in the intermediate and ventral hippocampus), grid cells with larger spacing than reported so far may be required.

the place field. Note that the weight only depends on the grid-cell spacing as all orientations are weighted equally, and that elementary calculus gives that the largest weight occurs for grid cells with a spacing $\lambda_{max} = 2\pi\sigma/\sqrt{3} \approx 3.6\sigma$.

In the following we consider a dorsal hippocampal place cell with a small place field ($\sigma = 12$ cm) with $f^{max} = 20$ Hz. In the sums we set $\lambda_{lower} = 28$ cm and $\lambda_{upper} = 73$ cm. This corresponds to the range of spacings observed in grid cells sampled from the most dorsal 25% of MEC (Hafting et al., 2005), which more or less corresponds to the area of MEC that provides input to any single place cell in the dorsal hippocampus (Witter, 1993; Dolorfo and Amaral, 1998; Naber et al., 2001). C_{inh} was set to balance the spatially constant excitatory contribution.

We first investigated whether the model is able to produce spatially confined place fields from a biologically plausible number of grid cells. A place field was defined as a continuous region of at least 200 cm^2 consisting of bins that exceed a firing rate of 20% of the cell's peak firing rate (Muller et al., 1987; Fyhn et al., 2004). We considered samples of 1,000 place cells for four different situations distinguished by the number (4, 10, 20, and 50) of grid-cell inputs. Only a single phase was considered, the orientation of each grid input was selected randomly with uniform sampling, and the grid spacing was selected randomly with logarithmic sampling between 28 and 73 cm. The weight for each grid-cell input was set according to Eq. (3) (Fig. 1C). The proportion of place cells with a single place field was calculated for each of the four model situations in small, medium-sized, and large environments (1 × 1, 4 × 4, and 10 × 10 m^2 quadratic arenas), mimicking the variation in size of environments encountered by rats in their natural habitat (Fig. 2).

The number of grid-cell inputs needed to produce a single place field increased with the size of the arena. In a typical laboratory recording arena (1 × 1 m^2), 10 randomly selected grid-cell inputs produced a single field for 781 out of the 1,000 place cells. For the largest arena considered (10 × 10 m^2), 20 randomly selected grids produced a single field in about a quarter of the place cells, but with input from 50 grid cells, all 1,000 place cells exhibited a single firing field in this environment (Fig. 2, pie charts). However, if the grid-cell parameters are set appropriately (typically with a high variation of spacing and orientation), single place fields could be formed with even fewer inputs, i.e., 4 inputs in the 1 × 1 m^2 arena, 10 inputs in the 4 × 4 m^2 arena, and 20 inputs in the 10 × 10 m^2 arena (Fig. 2, rate maps). Note that the example rate maps in Figure 2 have peak rates of about 12 Hz, significantly less than $f^{max} = 20$ Hz. This is mainly because of the restricted range of spacings (28–73 cm) considered, not the finite number of contributing grids. Summation (integration) over infinitely many grid inputs within this range yields a maximum firing rate of 12.2 Hz. Considering that the average number of anatomical connections between a grid cell and a place cell may be somewhere between 100 and 1,000 depending on how many contacts each grid cell makes with each place cell (Amaral et al., 1990; Rapp et al., 2002), these results suggest that linear summation of grid-cell inputs can reliably form unique hippocampal place fields in most of the environments explored by the animal.

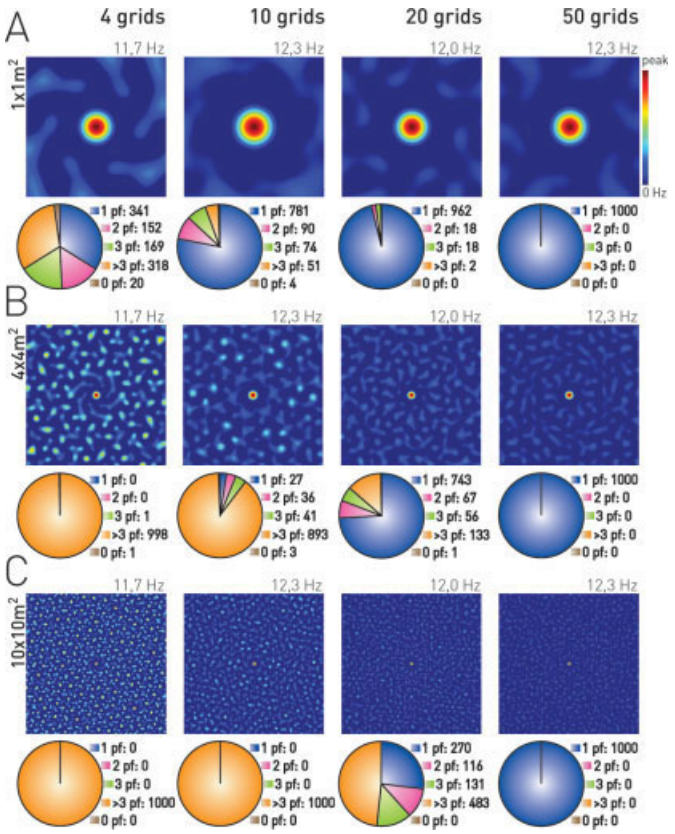

FIGURE 2. A small number of grid-cell inputs is sufficient for place field formation in the hippocampus. Example place-field rate maps and pie charts of place-field structure are shown for four situations with $N = 4$, 10, 20, or 50 grid cells providing input to the place cell in arenas of (A) 1 × 1 m^2, (B) 4 × 4 m^2, and (C) 10 × 10 m^2. Pie charts show the proportion of cells with different numbers of place fields (pf) in samples of 1,000 simulated place cells summing input from grid cells with identical spatial phases, random orientations, and random (logarithmically sampled) spacings between 28 and 73 cm, i.e., Eq. (1) with grid-cell functions and weights taken from Eqs. (2) and (3), respectively. Rate maps show example place cells with single fields except for $N = 4$ in the 4 × 4 m^2 arena and $N = 4$ and 10 in the 10 × 10 m^2 arena where no single-field examples were found. Note that four grid cells were sufficient to generate unique place fields in the 1 × 1 m^2 arena and that 20 grid cells were sufficient in the 10 × 10 m^2 arena. A few of the sums failed to produce a place field according to our criterion (i.e., a continuous region of at least 200 cm^2 consisting of bins that exceed a firing rate of 20% of the cell's peak firing rate). Peak rate is indicated on each rate map.

The grid cells exciting a place cell when the rat is in the place field of the cell are likely to exhibit some variation in spatial phase, i.e., their grid vertices may not be identical. To examine the amount of phase jitter tolerated by the model, we studied several samples of 1,000 place cells generated with $N = 20$ and $N = 50$ grid-cell inputs with various amounts of jitter in the spatial phase. As before, each grid cell was assigned a random orientation and a random spacing between 28 and 73

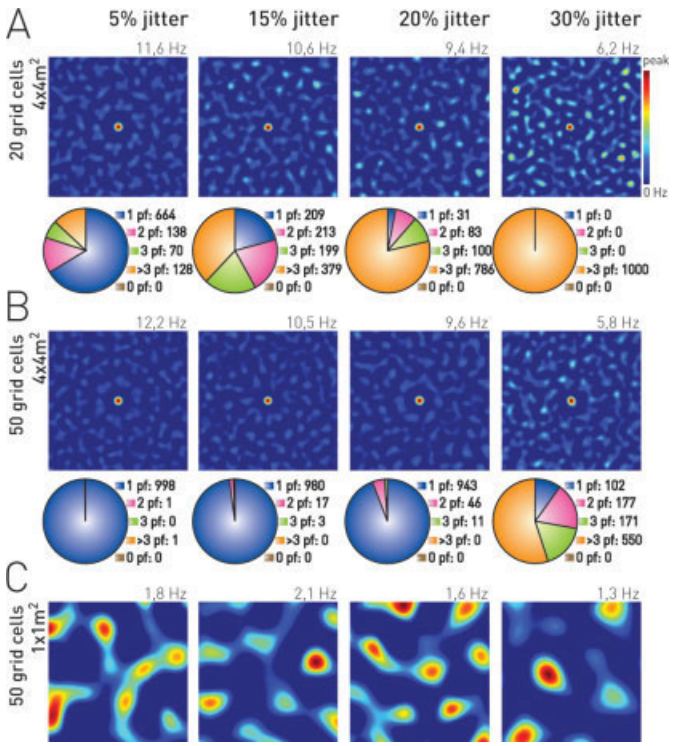

FIGURE 3. Hippocampal place cells tolerate some jitter in the spatial phase of the afferent grid cells. Each pie chart shows the proportion of cells with various numbers of place fields (pf) in a sample of 1,000 simulated place cells summing input from grid cells in a 4 × 4 m^2 arena. Each grid cell was assigned a random orientation, a random spacing within 28 and 73 cm, and a random spatial phase with different amounts of maximal deviation from the central peak (deviations of 5, 15, 20, and 30% of the grid spacing). In A and B, rate maps show example place cells from the category with the largest number of cells in the respective pie charts. Peak rate is indicated on each rate map. (A) 20 grid-cell inputs. (B) 50 grid-cell inputs. (C) Example rate maps for model with 50 grid-cell inputs with completely random spatial phases in a 1 × 1 m^2 arena.

cm, weighted as in Eq. (3) (Fig. 1C). In addition, spatial phase was picked randomly within a predefined range. Specifically, the spatial position ($\boldsymbol{r}_0$) of the relevant grid-cell peak was, for each of the contributing grid cells, randomly selected from a uniform distribution within a particular radius (0, 5, 10, ... 30% of the spacing) around the ideal position. We considered the 4 × 4 m^2 arena and calculated the proportion of place cells with a single place field in each condition. The model still produced localized place fields provided the variation of the spatial phase was not too large (Fig. 3A,B). With $N = 20$ inputs, 5% phase jitter still gave a single place field about two thirds of the time, which is only slightly lower than for the single-phase samples (75%; Fig. 2). Furthermore, with $N = 50$ inputs, a single place field was produced in about 95% of the place cells even with 20% phase jitter. Thus the phase-jitter tolerance is quite high, but the exact tolerance depends on the number of grid cells contributing to the field. When the spatial phase of the afferent grid cells was chosen completely at random, rate maps with multiple poorly defined and scattered place fields and very low peak rates were produced (Fig. 3C).

Because grid cells recorded at the same dorsoventral level of the MEC share a common orientation (Hafting et al., 2005; Sargolini et al., 2006), it is *a priori* possible that place cells receive the majority of their spatial inputs from grid cells with a similar grid orientation. However, this would result in place fields with hexagonally symmetric spokes protruding from the central peak (Fig. 4A). Inclusion of spatial-phase variation of the grids does not mitigate this effect (Fig. 4B). If place fields were formed from grid cells with diverse orientations but similar spatial phases and spacings, the size of the central field would be similar to that of the projecting grid cells, but a circular pattern of extra-field activity would appear unless strong inhibition is present (Fig. 4C). Inclusion of variation in the spatial phase would not remove the ring effect (Fig. 4D). The possibility of a common spacing for all inputs to a hippocampal place cell is also improbable from an anatomical view point, since principal cells in the hippocampus receive convergent input from a significant portion of the dorsoventral axis of the EC (Witter, 1993; Dolorfo and Amaral, 1998; Naber

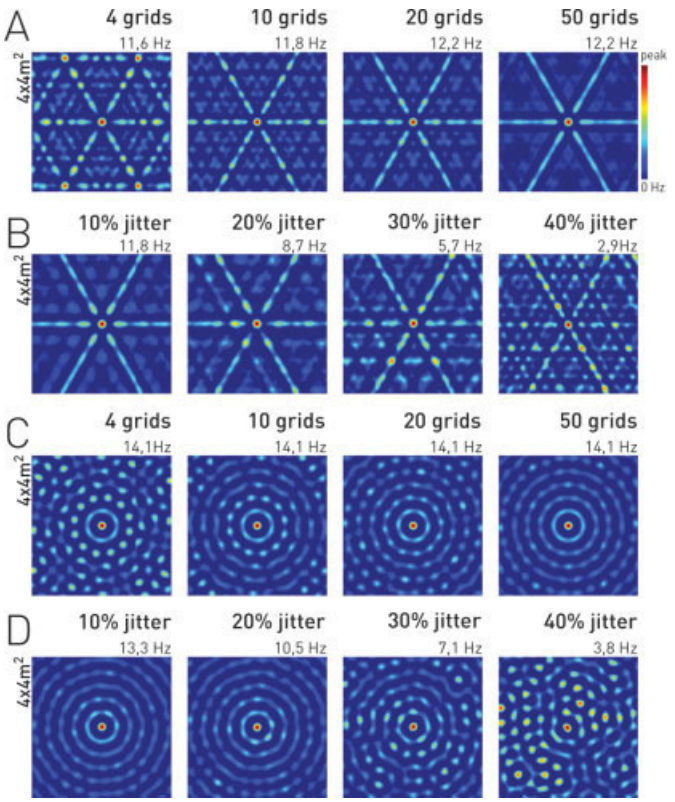

FIGURE 4. Hippocampal place fields may require inputs covering a diversity of grid orientations and grid spacings. (A) Input from grid cells with a single phase and a single orientation only ($\Theta = 0^\circ$). (B) 50 grid-cell inputs with single orientation ($\Theta = 0^\circ$) as in A, but with different amounts of spatial phase jitter. (C) Input from grid cells with a single phase and a single spacing only ($\lambda = \lambda_{max} = 43.5$ cm). (D) Fifty grid-cell inputs with single spacing as in C ($\lambda = \lambda_{max} = 43.5$ cm), but with different amounts of spatial phase jitter. Peak rate is indicated on each rate map.

et al., 2001) and, by implication, from entorhinal cells with a broad range of grid spacings (Hafting et al., 2005; Sargolini et al., 2006).

The weight function in Eq. (3) is based on the assumption of a Gaussian place field and a logarithmic sampling of grid spacings (Supplementary material, Section 2). Even though this choice of sampling is irrelevant for the resulting sum if the discretization is sufficiently dense, the choice will matter somewhat when the number of grid-cell inputs is small. Nevertheless, exploration of models with non-Gaussian weights, e.g., constant $A_{\mathbf{w0}}$ for spacings between λ_{lower} and λ_{upper}, and linear, instead of logarithmic, sampling still produced confined place fields with roughly the same proportion of single fields as considered in Figure 2 (data not shown). This implies that even if the weight distribution for the grid-cell inputs does not follow Eq. (3), singly confined place fields will still be formed as long as the place cells sample a sufficiently wide range of grid spacings and a multitude of orientations.

Taken together, these simulations show that confined place fields can be reliably formed by dendritic summation of appropriately weighted inputs from a relatively low number of simultaneously active grid cells covering a range of spacings and a diversity of orientations. Place fields emerge from augmentation of a central peak and cancellation of surrounding peaks in grid-cell patterns with different scale and orientation, but relatively similar spatial phase. The concept of transformation from grid fields to place fields by linear summation has been proposed earlier (O'Keefe and Burgess, 2005; McNaughton et al., 2006), but the present mathematical model provides new insight into the parameters of grid fields determining the formation of place fields and the consequences of biologically plausible variation in each of these parameters.

First, the model points to integration across a moderate range of grid spacings as an essential condition for place field formation in the hippocampus. To integrate inputs from grid cells with different spacings, each place cell must be innervated by cells from different dorsoventral levels of the MEC (Fig. 1). Such a wiring scheme is supported by the topographical organization of the connections between EC and hippocampus. A typical stellate or pyramidal cell in the EC projects to roughly 25% of the dorsoventral axis of the hippocampus in such a way that the overlap between the most dorsal and the most ventral projections is virtually zero (Dolorfo and Amaral, 1998; Witter and Amaral, 2004). The increase in grid spacing along the dorsoventral axis of the MEC can account for the increase in place-field size along the dorsoventral axis of the hippocampus (Kjelstrup et al., 2006; Fig. 1A). This also points to one way of testing the model, as it implies broader place fields in the hippocampus in response to inactivation of the dorsal MEC and more focused place fields in response to inactivation of the ventral MEC (Supplementary material, Section 3).

Second, if a place cell is innervated by grid cells with similar grid orientations, the model predicts a hexagonal spoke pattern appearing around the place field (Fig. 3A). Because there is no experimental support for such spatial regularities in out-of-field firing in hippocampal place cells, the spokes must either be hidden by strong inhibition or high firing-rate thresholds, or place cells must be innervated by grid cells with a broad range of grid orientations. The latter alternative is supported by recent observations indicating that grid orientation varies between different regions of the MEC, at least between grid cells in different hemispheres (Hafting et al., 2005; Fyhn et al., 2006). How grid cells with different grid orientation are mapped across the entorhinal surface remains to be determined, however.

Third, the simulations imply that, although some jitter is tolerated, place fields may be generated predominantly by inputs from grid cells with overlapping vertices centered at the place field, i.e., grid cells with similar spatial phases. The temporally clustered firing of cells with overlapping grid fields is consistent with the fact that strong perforant path stimulation is consistent required to elicit spikes from CA1 neurons in vitro (Jarsky et al., 2005). Multiple place fields arise in the model if the place cell is innervated by two or more groups of grid cells where the spatial phases are similar within each group but dissimilar between the groups. Without coherence in spatial phase, disordered firing-rate maps emerge (Fig. 3C), resembling those of neurons in the dentate gyrus (Jung and McNaughton, 1993). This implies a possible role for spatial phase selectivity in explaining differences between the hippocampal areas.

The hippocampal place code can undergo substantial changes, referred to as "remapping," in response to only minor alterations in the sensory or motivational inputs to the hippocampal formation (Muller and Kubie, 1987; Quirk et al., 1990; Leutgeb et al., 2004, 2005; Wills et al., 2005). When the input changes sufficiently to induce a complete reorganization of the place representation "global remapping"; Leutgeb et al., 2005), the remapping is accompanied by a significant shift and reorientation of the entorhinal grid-cell representation (Fyhn et al., 2006). Our model only addresses established hippocampal representations, but because the number of entorhinal cells with projections to a given place cell (~100–1,000; Amaral et al., 1990; Rapp et al., 2002) is likely to significantly outnumber the grid-cell inputs required to form a place field in our model (~10–50), the study suggests that remapping may often be associated with a replacement of the set of grid cells driving a given place cell. The mechanism of this replacement is beyond the scope of the present study.

In conclusion, this work supports the plausibility of a model for how hippocampal place fields are formed by integration of grid-cell inputs, where (i) the hippocampal neurons sum synaptic inputs in an approximately linear manner, (ii) a modest number (<50) of afferent grid cells are required in each environment, and (iii) the grid cells providing the inputs sample a significant range of grid spacings and grid orientations, but a limited set of spatial phases.

Acknowledgments

The authors thank May-Britt Moser, Alessandro Treves, Menno Witter, John Lisman, Marianne Fyhn, Torkel Hafting, Dori Derdikman, and Espen J. Henriksen for discussion and comments on earlier versions of the manuscript.

REFERENCES

Amaral DG, Ishizuka N, Claiborne B. 1990. Neurons, numbers and the hippocampal network. Prog Brain Res 83:1–11.

Cash S, Yuste R. 1998. Input summation by cultured pyramidal neurons is linear and position-independent. J Neurosci 18:10–15.

Cash S, Yuste R. 1999. Linear summation of excitatory inputs by CA1 pyramidal neurons. Neuron 22:383–394.

Dolorfo CL, Amaral DG. 1998. Entorhinal cortex of the rat: Topographic organization of the cells of origin of the perforant path projection to the dentate gyrus. J Comp Neurol 398:25–48.

Fyhn M, Molden S, Witter MP, Moser EI, Moser MB. 2004. Spatial representation in the entorhinal cortex. Science 305:1258–1264.

Fyhn MH, Hafting TF, Treves A, Moser EI, Moser MB. 2006. Coherence in ensembles of entorhinal grid cells. Soc Neurosci 68.9/BB17.

Gasparini S, Magee JC. 2006. State-dependent dendritic computation in hippocampal CA1 pyramidal neurons. J Neurosci 26:2088–2100.

Hafting T, Fyhn M, Molden S, Moser MB, Moser EI. 2005. Microstructure of a spatial map in the entorhinal cortex. Nature 436:801–806.

Jarsky T, Roxin A, Kath WL, Spruston N. 2005. Conditional dendritic spike propagation following distal synaptic activation of hippocampal CA1 pyramidal neurons. Nat Neurosci 8:1667–1676.

Jung MW, McNaughton BL. 1993. Spatial selectivity of unit activity in the hippocampal granular layer. Hippocampus 3:165–182.

Jung MW, Wiener SI, McNaughton BL. 1994. Comparison of spatial firing characteristics of units in dorsal and ventral hippocampus of the rat. J Neurosci 14:7347–7356.

Kjelstrup KG, Solstad T, Brun VH, Fyhn M, Hafting T, Leutgeb S, Witter MP, Moser MB, Moser EI. 2006. FENS Forum R11641.

Leutgeb S, Leutgeb JK, Barnes CA, Moser EI, McNaughton BL, Moser MB. 2005. Independent codes for spatial and episodic memory in hippocampal neuronal ensembles. Science 309:619–623.

Leutgeb S, Leutgeb JK, Treves A, Moser MB, Moser EI. 2004. Distinct ensemble codes in hippocampal areas CA3 and CA1. Science 305:1295–1298.

Maurer AP, Vanrhoads SR, Sutherland GR, Lipa P, McNaughton BL. 2005. Self-motion and the origin of differential spatial scaling along the septo-temporal axis of the hippocampus. Hippocampus 15:841–852.

McNaughton BL, Battaglia FP, Jensen O, Moser EI, Moser MB. 2006. Path integration and the neural basis of the "cognitive map." Nat Rev Neurosci 7:663–678.

Muller RU, Kubie JL. 1987. The effects of changes in the environment on the spatial firing of hippocampal complex-spike cells. J Neurosci 7:1951–1968.

Muller RU, Kubie JL, Ranck JB Jr. 1987. Spatial firing patterns of hippocampal complex-spike cells in a fixed environment. J Neurosci 7: 1935–1950.

Naber PA, Witter MP, Lopes da Silva FH. 2001. Evidence for a direct projection from the postrhinal cortex to the subiculum in the rat. Hippocampus 11:105–117.

O'Keefe J, Burgess N. 1996. Geometric determinants of the place fields of hippocampal neurons. Nature 381:425–428.

O'Keefe J, Burgess N. 2005. Dual phase and rate coding in hippocampal place cells: Theoretical significance and relationship to entorhinal grid cells. Hippocampus 15:853–866.

O'Keefe J, Dostrovsky J. 1971. The hippocampus as a spatial map. Preliminary evidence from unit activity in the freely-moving rat. Brain Res 34:171–175.

O'Keefe J, Nadel L. 1978. The Hippocampus as a Cognitive Map. Oxford: Clarendon. 570 p.

Quirk GJ, Muller RU, Kubie JL. 1990. The firing of hippocampal place cells in the dark depends on the rat's recent experience. J Neurosci 10:2008–2017.

Rapp PR, Deroche PS, Mao Y, Burwell RD. 2002. Neuron number in the parahippocampal region is preserved in aged rats with spatial learning deficits. Cereb Cortex 12:1171–1179.

Riley KF, Bence SJ, Hobson MP. 2006. Mathematical Methods for Physics and Engineering. Cambridge: Cambridge University Press. 1333 p.

Sargolini F, Fyhn M, Hafting T, McNaughton BL, Witter MP, Moser MB, Moser EI. 2006. Conjunctive representation of position, direction, and velocity in entorhinal cortex. Science 312:758–762.

Wills TJ, Lever C, Cacucci F, Burgess N, O'Keefe J. 2005. Attractor dynamics in the hippocampal representation of the local environment. Science 308:873–876.

Wilson MA, McNaughton BL. 1993. Dynamics of the hippocampal ensemble code for space. Science 261:1055–1058.

Witter MP. 1993. Organization of the entorhinal-hippocampal system: A review of current anatomical data. Hippocampus 3 Spec No: 33–44.

Witter MP, Amaral DG. 2004. The hippocampal formation. In: Paxinos G, editor. The Rat Nervous System, 3rd ed. New York: Elsevier.